



## Research Article

# Comparative Assessment of Various Formats of TRAIL in Three-Dimensional Cell Culture and Patient-Derived Tumoroids of Colorectal Cancer

Farzaneh Vafaeinik<sup>1</sup>, Sarah Helmueller<sup>1</sup>, Alexandra Gangi<sup>2</sup>, Ja-Lok Ku<sup>3</sup>, Roland Kontermann<sup>4</sup>, Yong J. Lee<sup>1\*</sup>

<sup>1</sup>Department of Biomedical Sciences, Cedars-Sinai Medical Center, Los Angeles, CA 90048, USA.

<sup>2</sup>Department of Surgery, Cedars-Sinai Medical Center, Los Angeles, CA 90048, USA.

<sup>3</sup>Department of Biomedical Sciences/Department of Medicine, Laboratory of Cell Biology, Cancer Research Institute, College of Medicine, Seoul National University, Seoul, Korea.

<sup>4</sup>Institute of Cell Biology and Immunology, University of Stuttgart, Stuttgart, Germany.

**\*Corresponding author:** Yong J. Lee, Department of Biomedical Sciences, Cedars-Sinai Medical Center, Los Angeles, CA 90048, USA.

**Citation:** Vafaeinik F, Helmueller S, Gangi A, Ku JL, Kontermann R, et al. (2025) Comparative Assessment of Various Formats of TRAIL in Three-Dimensional Cell Culture and Patient-Derived Tumoroids of Colorectal Cancer. J Oncol Res Ther 10: 10302. DOI: 10.29011/2574-710X.10302

**Received Date:** 26 August, 2025; **Accepted:** 09 September, 2025; **Published Date:** 12 September, 2025

## Abstract

Tumor necrosis factor-related apoptosis-inducing ligand (TRAIL) has emerged as a promising cytokine that selectively targets cancer cells while sparing normal tissues. Despite its favorable safety profile, clinical trials have demonstrated antitumor responses in only a small subset of patients. This limited efficacy has been largely attributed to the short plasma half-life of recombinant monomeric soluble TRAIL (rhTRAIL). To enhance its stability and therapeutic potential, researchers have developed modified versions, including an immunoglobulin Fc domain-fused TRAIL (Fc-TRAIL) and a dimeric Fc-fused single-chain variant (Fc-scTRAIL). In this study, we used the SNU-1746 three-dimensional (3D) multicellular layer culture model and a patient-derived colon cancer tumoroid model to evaluate the biological activity of these TRAIL formats (rhTRAIL, Fc-TRAIL, and Fc-scTRAIL). Treatment with rhTRAIL revealed that a longer exposure time (18-24 hours) was required to induce apoptosis in both 3D models, in contrast to monolayer cultures. Among the TRAIL formats, Fc-scTRAIL was the most potent in inducing apoptosis, as confirmed by immunoblotting analyses. Furthermore, artesunate (ART) enhanced TRAIL-induced apoptosis across all TRAIL formats, with the strongest synergistic effect observed in combination with Fc-scTRAIL. JC-1 staining assays indicated that mitochondrial membrane depolarization (a hallmark of the intrinsic apoptosis pathway) plays a key role in the cell death observed with the combination treatment in tumoroids. These findings provide compelling preclinical evidence supporting the potential of ART and Fc-scTRAIL combination therapy for future clinical evaluation.

## Introduction

Colorectal cancer (CRC) is a significant malignancy that arises from glandular cells, typically progressing from benign polyps to invasive cancer over a span of 5 to 15 years. It is the second leading cause of cancer-related mortality, following lung cancer [1]. CRC exhibits several key characteristics, including elevated

metabolic activity, accelerated cell division, and increased invasive potential [2]. Current treatment options include chemotherapy, radiation therapy, surgery, immunotherapy, and targeted therapies. However, the cost of colon cancer treatment is high and expected to rise further [3]. While chemotherapy plays a central role in cancer treatment, drugs such as 5-fluorouracil, hydroxyurea,

and platinum-based compounds often cause significant side effects, highlighting the need for more targeted and less harmful therapeutic approaches [1].

TRAIL (tumor necrosis factor-related apoptosis-inducing ligand), also known as APO2L, is a type II integral membrane protein belonging to the tumor necrosis factor (TNF) family [4]. TRAIL consists of 281 and 291 amino acids in the human and murine forms, respectively, related most closely to a Fas/APO-1 ligand [4, 5]. Like Fas ligand (FasL) and TNF, the COOH-terminal extracellular region of TRAIL (amino acids 114-281) exhibits a homotrimeric subunit structure and interacts with TRAIL death receptors [5]. TRAIL-induced apoptosis can be initiated via the death receptor (extrinsic) pathway and the subsequent mitochondrial (intrinsic) pathway with divergent death signals activated by different stimulators [6]. TRAIL initiates the extrinsic pathway by binding to death receptors (DRs) such as DR4 (TRAIL-R1) and DR5 (TRAIL-R2) and inducing the apoptotic signal by recruiting Fas-associated protein with death domain (FADD) via death domain (DD) interactions [7]. However, in normal cells TRAIL also binds to highly expressed three decoy receptors (DcR1, DcR2, and osteoprotegerin), which may result in inhibition of TRAIL signaling [8, 9]. Both DR4 and DR5 have extracellular, transmembrane, and cytoplasmic domains. TRAIL-induced activation of cytoplasmic DDs leads to formation of the death-inducing signaling complex (DISC) [10]. Initiator caspase-8 and -10 recruitment and activation at the DISC leads to further activation of signaling molecules downstream, which results in activation of executioner caspase-3, -6, and -7 and culminates in apoptotic death [11]. Activated caspase-8 can also cleave the pro-apoptotic protein Bid into truncated Bid (tBid), which is a membrane-targeted death ligand. When translocated to the mitochondria, tBid induces Bax and Bak oligomerization [12, 13]. Insertion of oligomerized Bax and Bak into the mitochondrial outer membrane, followed by permeabilization and depolarization of the mitochondria lead to cytochrome c release [14, 15]. When cytochrome c enters the cytosol, it facilitates the formation of the apaf1 (apoptosis signal-regulating kinase)/caspase-9 apoptosome, which activates caspase-9 and subsequently caspase-3 [16].

TRAIL has emerged as a potential anticancer agent due to its ability to induce apoptosis in cancer cells with minimal toxicity to normal tissues [17]. However, its use has been constrained by challenges such as low bioavailability, short half-life, and tumor resistance [18]. To address these challenges, modified TRAIL formats—such as Fc-fusions and nanoparticle-conjugated TRAIL, and antibody-linked constructs have been developed to enhance tumor targeting, and apoptotic efficacy [19]. Studies on the pharmacokinetics of TRAIL reveal that intravenous bolus injected TRAIL protein is rapidly eliminated from the serum [20]. In addition, many human tumors resist TRAIL-induced apoptosis [21-23]. To overcome these

limitations, several researchers have developed various formats of TRAIL. Dr. Wu's group developed an immunoglobulin Fc domain-fused TRAIL (Fc-TRAIL) protein. This chimeric protein displays higher specific activity in vitro, efficient therapeutic activity in vivo, and a significantly longer plasma half-life without hepatic toxicity [24]. Dr. Kontermann's group also developed dimeric Fc-scTRAIL protein containing the fragment crystallizable region Fc of a human immunoglobulin-fused single-chain version of TRAIL [25, 26]. A single-chain TRAIL (scTRAIL) moiety consisting of three TRAIL protomers (aa 118-281) linked by glycine residues is used as a building block to create dimeric scTRAIL fusion proteins. Dimeric scTRAIL proteins are generated by fusing scTRAIL to the C-terminus of a human IgG1 immunoglobulin Fc domain (Fc-scTRAIL). Dimeric Fc-scTRAIL increases the plasma half-life of the fusion protein [27]. Previous studies have demonstrated that the presence of the Fc domain prolongs therapeutic activity in vivo through its interaction with the neonatal Fc receptor and slower renal clearance [15, 28].

Although TRAIL is known for its ability to induce apoptosis selectively in cancer cells, many tumors, especially highly aggressive tumors, exhibits resistance to TRAIL-induced apoptosis. Combining TRAIL with chemotherapy or radiotherapy has been shown to sensitize resistant tumors to TRAIL, but such combinations often cause significant toxicity to healthy cells [29]. To overcome TRAIL resistance and enhance its therapeutic potential, there is a growing focus on combining TRAIL with other effective antitumor agents. Among these, artesunate (ART), a semi-synthetic derivative of artemisinin, stands out as a promising candidate. In recent years, artemisinin and its derivatives have proven to be highly effective and safe for treating severe, chloroquine-resistant malaria [29, 30]. Several studies have demonstrated that ART inhibits multiple signaling pathways involved in tumor progression. These effects include the inhibition of cell proliferation, activation of various forms of tumor cell death, and the reduction of angiogenesis, invasion, and metastasis [31, 32]. Although artemisinin derivatives have demonstrated anti-tumor effects in preclinical models, their clinical effectiveness remains limited [31]. To better understand their therapeutic potential, this study examined ART alone and in combination with standard chemotherapies using clinically relevant concentrations in advanced three-dimensional (3D) models, which closely replicate the complexity and treatment response of colorectal cancer. The two-dimensional (2D) culture system is commonly considered a low-cost and easy-to-use in vitro model for large-scale cultivation and harvesting of human and animal cells [33]. So far, 2D cell culture models have been widely used in drug discovery. However, they do not adequately represent the structural complexity, cellular heterogeneity, or environmental conditions of living tissues. A major limitation to the physiological relevance of 2D cultures is

the interaction between cells and their surrounding extracellular matrix (ECM). The ECM's biochemical and mechanical properties are essential for maintaining homeostasis and can impact drug responses by affecting efficacy, resistance, or mechanisms of action [34]. Recently, there has been a shift in cancer drug development towards using 3D culture models, which provide a more accurate representation of tumor behavior and characteristics compared to conventional 2D models [35]. Moreover, in this study, we employed a CRC patient-derived tumoroid model which offers several major advantages. Tumoroids retain the genetic, histological, and molecular features of the original tumors which leads to more physiologically relevant responses [36]. These models replicate key tumor features, including gradients of oxygen, nutrients, and proliferation, and have been successfully applied in drug screening to identify effective cancer therapies [34]. In this study, we compared four different formats of TRAIL, recombinant human soluble TRAIL (aa 114-281: rhTRAIL), Fc domain-fused TRAIL (aa 95-281: Fc-TRAIL), single-chain TRAIL (three aa 118-281:scTRAIL), and Fc domain-fused single-chain TRAIL (three aa 118-281:Fc-scTRAIL),-induced apoptosis in SNU-1746 3D spheroid cultures and CRC tumoroids. We observed that Fc-scTRAIL was the most effective in inducing apoptosis.

Furthermore, we investigated, for the first time, the combinatorial effects of ART with various formats of TRAIL, including rhTRAIL, Fc-TRAIL, and Fc-scTRAIL, in CRC tumoroids. Notably, the combination of Fc-scTRAIL and ART markedly enhanced apoptosis in these complex 3D models. These results suggest that combining ART with TRAIL-based therapies may offer a promising strategy for colorectal cancer treatment.

## Materials and Methods

### Cell Lines and Cell Culture Conditions

The human colon adenocarcinoma SNU-1746 line was obtained from Korean Cell Line Bank (Seoul, Korea). The KCLB routinely performs quality control measures—including mycoplasma contamination tests—on all cell lines prior to distribution. These cells were maintained in RPMI 1640 medium with 10% fetal bovine serum, 25 mM HEPES buffer, 25 mM sodium bicarbonate, and L-glutamine (300 mg/L). These cells were incubated in a humidified atmosphere of 5% CO<sub>2</sub> at 37°C.

### Chemicals and Reagents

We produced human recombinant rhTRAIL as previously described [37]. In brief, human TRAIL cDNA fragment (amino acids 114–281) was obtained by reverse transcription-PCR and then cloned into a pET-23d (Novagen, Madison, WI) plasmid. We used the Qiagen express protein purification system (Qiagen, Valencia, CA) to purify His-tagged TRAIL protein. We produced human Fc-TRAIL as previously described [24]. In brief, the

Fc-TRAIL cDNA was generated by overlapping fragments of human immunoglobulin Fc domain (amino acids 6-323) cDNA and TRAIL (amino acids 95-281) and then cloned into a pET28a (Novagen, Madison, WI) plasmid. We used the Qiagen express protein purification system (Qiagen, Valencia, CA) to purify His-tagged Fc-TRAIL protein. We produced human scTRAIL and Fc-scTRAIL as previously described [26]. In brief, a single-chain TRAIL (scTRAIL) moiety consisting of three TRAIL protomers (aa 118-281) linked by glycine residues was cloned into a pET28a plasmid, Fc-scTRAIL was cloned into a pSecTagA (Invitrogen, Thermo Fisher Scientific, V90020) plasmid. We used the Qiagen express protein purification system (Qiagen, Valencia, CA) to purify His-tagged scTRAIL protein. We stably transfected pSecTagA containing Fc-scTRAIL plasmid into DR5 knock-out HEK293T cells (Synthego Corp., Redwood City, CA) and cultivated the HEK293T cells in Opti-MEM (Thermo Fisher Scientific, 31985–070) containing 50 µmol/L ZnCl<sub>2</sub> and then purified Fc-scTRAIL protein from the supernatant via FLAG affinity chromatography. Artesunate (catalog A3731) and N-Acetyl-L-cysteine (NAC) (catalog A7250) were bought from Sigma-Aldrich (St. Louis, MO, USA). Human EGF Recombinant Protein (catalog PHG0311), Gibco™ DMEM/F-12, GlutaMAX™ (catalog 10-565-018), Human R-Spondin 1 Recombinant Protein (catalog 120-38-100UG), B27 Supplement (catalog 17-504-044), and Recombinant Human Noggin (catalog PHC1506) were bought from Fisher Scientific (Waltham, MA, USA). Y-27632 (catalog 1254) was purchased from Tocris Bioscience (Bristol, UK). Servator B Storage Solution was purchased from Global Transplant Solutions Inc. (Spartanburg, SC, USA).

### Isolation of Tumor Tissue

Fresh tissue samples of malignant neoplasm of the sigmoid colon were obtained from a low anterior resection surgery performed by Dr. Alexandra Gangi at Cedars-Sinai Medical Center. Tumor tissues were stored in Servator B Storage Solution in a 50 mL tube at 4°C for 24 hours to successfully process them the next day.

To isolate tumor tissues, first, tissue samples were transferred into a petri dish containing ice-cold Dulbecco's Phosphate Buffered Saline without Ca<sup>2+</sup> and Mg<sup>2+</sup> (DPBS) using sterile forceps, and washed with cold DPBS to remove blood and debris. Tumor tissues were minced into small pieces using sterilized scissors and forceps. The minced tissue was then transferred to a strainer (Falcon cell strainer) placed on top of a 50 mL tube (cold DPBS was added to facilitate the transfer of all minced tissue). The tissue pieces were further minced and ground through the strainer using a 5 mL syringe plunger. After collecting the sample into a 50 mL conical tube with DPBS, it was centrifuged at 1000 × g for 5 minutes. Then, we carefully aspirated out the DPBS after pelleting and resuspended the tissue in 5 mL of ACK Blood Lysis Buffer,

and incubated for 10-15 minutes at room temperature. The tissue samples mixed with the buffer were centrifuged at  $1000 \times g$  for 5 minutes. After repeating the Lysis buffer step 1-2 more times, the tissue color changed to white, indicating the reduction of red blood cells in the tissue. The tissue samples were washed 3-4 times with freshly prepared 2mM EDTA chelation buffer (consisting of 2% sorbitol, 1% sucrose, 1% bovine serum albumin fraction V (BSA), and 1x Gentamicin/Amphotericin solution in Dulbecco's Phosphate Buffered Saline without  $Ca^{2+}$  and  $Mg^{2+}$  (DPBS), filter sterilized with a 0.22  $\mu m$  filter (500 mL)). The samples were centrifuged at  $1000 \times g$  for 5 minutes, then incubated on ice for 1 hour on a horizontal orbital shaker. Afterward, they were centrifuged again, and the tissues were washed 3-4 times with ice-cold chelation buffer without EDTA. They were then centrifuged at  $1000 \times g$  for 5 min. The tissue pellets were resuspended in 15-20 mL of digestion buffer (supplemented with 2.5% fetal bovine serum, 1 unit/mL penicillin, 1  $\mu g/mL$  streptomycin, 2.5 ng/mL amphotericin B, 200 U/mL type IV collagenase, and 125  $\mu g/mL$  type II dispase in Dulbecco's Modified Eagle Medium) and transferred into a T25 flask to incubate for 2 hours at 37°C. After incubation, the suspension was filtered through a small strainer (Falcon cell strainer) into a 50 mL tube. After another round of centrifugation, the pellet was resuspended in ice-cold chelation buffer and centrifuged again to discard the supernatant. Then, isolated tumor cells were used for subsequent culture.

### Establishment of Tumoroid Formation

After thawing 1-2 mL of Matrigel on ice, complete cell culture medium (DMEM/F-12 + GlutaMAX medium, R-spondin 1 (500 ng/mL), Noggin (100 ng/mL), EGF (50 ng/mL), A83-01 (0.2  $\mu M$ ), Y-27632 dihydrochloride (10  $\mu M$ ), B27 (50X), and 1.25 mM N-Acetylcysteine) was added to the Matrigel in a ratio of ~1:2 (medium to Matrigel). Isolated tumor cells were then resuspended in the Matrigel and transferred into a clean 50 mL tube through a Flowmi® Cell Strainer. Next, 100  $\mu L$  of the suspension was pipetted into the center of each well in a pre-incubated 12-well plate. The plate with tissue and Matrigel was incubated for 15 minutes at 37°C, inverted carefully, and then incubated for an additional 5 minutes. Finally, 1 mL of complete cell culture medium was carefully added to each well to submerge the tissue + Matrigel and incubated at 37°C.

### Passaging Tumoroid Embedded Culture

For passaging, the tumor-containing Matrigel dome was first taken out of the 12-well plate by breaking up the Matrigel through pipetting up and down with a P1000 pipette tip, and the Matrigel pieces, along with all medium, was transferred into a 15 mL tube. The tubes were then centrifuged at  $1000 \times g$  for 5 minutes. The supernatant was removed and discarded, and the tumoroid pellet was resuspended with 1 mL of trypsin containing Y-27632

dihydrochloride (10  $\mu M$ ) and incubated for 5 minutes at 37°C. After incubation, ~2 mL DMEM medium was added to the cells, and the suspension was spun down at  $1000 \times g$  for 5 minutes. The pellet was resuspended in diluted Matrigel (in a ratio of ~1:2, complete medium to Matrigel), and 100  $\mu L$  of the suspension was pipetted into the center of each well in a pre-incubated 12-well plate. After the plate was incubated for 15 minutes at 37°C, it was inverted and incubated for an additional 5 minutes. Finally, 1 mL of complete cell culture medium was added carefully to each plate and incubated at 37°C.

### Storage and Recovery of Tumoroids

For cryopreservation of tumoroids the tumor-containing Matrigel dome was first taken out of the 12-well plate by breaking up the Matrigel through pipetting up and down with a P1000 pipette tip, and the Matrigel pieces, along with all medium, was transferred into a 15 mL tube. The suspension was centrifuged at  $1000 \times g$  for 5 minutes at 2-8°C. The supernatant was removed and discarded, and the tumoroid pellet was resuspended in 1 mL of cold freezing medium composed of DMEM/F-12 + GlutaMAX, supplemented with 10% fetal bovine serum (FBS), 10% dimethyl sulfoxide (DMSO), and Y-27632 dihydrochloride (10  $\mu M$ ). The suspension was transferred into labeled cryovials and stored at -80°C overnight, followed by transfer to liquid nitrogen for long-term storage. For recovery, the frozen tumoroids were rapidly thawed in a 37°C water bath, pipetted into 5 mL of DMEM media in 15 mL tubes, and then centrifuged at  $1000 \times g$  for 5 minutes at 2-8°C. The tumoroid pellet was resuspended in cold Matrigel and plated under the culture conditions described above.

### PI and Hoechst staining and quantification of cytotoxicity

Tumoroids were cultured in a 12-well plate and treated as indicated. After treatment, they were washed with PBS to remove media and debris. A working solution of PI (Propidium Iodide Solution, Sigma-Aldrich, Cat. No. P4864) was prepared by diluting the stock solution to a final concentration of 50  $\mu g/mL$  in PBS. The solution was added directly to each well and incubated in the dark at room temperature for 30 minutes. After incubation, the cells were washed with PBS. Hoechst dye was then added by diluting the stock solution 1:2000 in PBS, followed by incubation at room temperature for 10-15 minutes in the dark. After staining, tumoroid morphology was observed under a fluorescence microscope, specifically the ECHO Revolve microscope (ECHO, San Diego, CA, USA). For cytotoxicity analysis, the mean fluorescence intensity (MFI) of PI and Hoechst staining was quantified using ImageJ software. MFI values were measured from at least three randomly selected fields for each experimental condition. The PI/Hoechst ratio was obtained by dividing the PI MFI by the Hoechst MFI in each field.



### **TUNEL Assay**

For detection of apoptosis using the terminal deoxynucleotidyl transferase dUTP nick end labeling (TUNEL) method, tumoroids were plated in a 12-well plate and treated as indicated. After treatment, they were washed once with phosphate-buffered saline (PBS). TUNEL reaction mixture was added to the samples and incubated at 37°C for 1 hour in the dark using the In Situ Cell Death Detection Kit, Fluorescein (Roche, cat # 11684795910), following the manufacturer's instructions. The tumoroids were then washed with PBS and examined under an ECHO fluorescence microscope. Cytotoxicity was analyzed by quantifying the mean fluorescence intensity (MFI) of TUNEL and Hoechst signals using ImageJ software. For each experimental condition, MFI values were measured from at least three randomly chosen fields. The TUNEL/Hoechst ratio was obtained by dividing the TUNEL MFI by the corresponding Hoechst MFI in each field.

### **JC-1 Assay**

To analyze mitochondrial membrane potential, the tumoroids were grown in a 12-well plate and treated as indicated. They were then stained using the JC-1 Mitochondrial Membrane Potential Assay Kit (JC-1 Dye, Thermo Fisher Scientific) according to the manufacturer's instructions and examined under an ECHO fluorescence microscope. Mitochondrial depolarization in tumoroids was evaluated by observing a shift from red to green fluorescence under a fluorescence microscope.

### **Cell Death Assay**

For fluorescence imaging, propidium iodide (PI) (Thermo Fisher Scientific, Waltham, TX) was used to stain dead cells. The nuclei of dead and live cells were counterstained with Hoechst 33342 (Thermo Fisher Scientific, Waltham, TX).

### **Western Blot Analysis and Antibodies**

Immunoblotting was carried out as previously described [38]. The following antibodies were used in this study: anti-PARP (#9532) from Cell Signaling Technology (Danvers, MA); and anti-actin, goat anti-rabbit IgG-horseradish peroxidase (HRP), and goat anti-mouse IgG-HRP from Santa Cruz Biotechnology (Dallas, TX).

### **Densitometry Analysis**

To quantify the relative protein level, western blot analyses from three different experiments were performed and densitometry analysis from the interesting bands was performed using the ImageJ program.

### **Combination Index Analysis**

The combination index (CI) was calculated using CompuSyn software (ComboSyn, Inc., Paramus, NJ, USA) to evaluate the degree of drug interaction—antagonism or synergism. CI values were interpreted as follows: CI values above 1 indicate antagonism between the drugs, whereas values below 1 denote synergy. CI values in the 0.9–1.10 range suggest an additive effect; those between 0.85–0.9 are interpreted as slight synergy; values between 0.3–0.7 point to moderate synergy; and those less than 0.3 indicate strong synergy.






### **Statistical Analysis**

All values are represented as mean  $\pm$  standard deviation (SD). Statistical analysis was performed using one-way analysis of variance or two-way analysis of variance followed by Tukey's post hoc test as indicated using GraphPad Prism 8 software. p values of less than 0.05 were defined as statistically significant. Significance of p value is indicated as \*P < 0.05; \*\*P < 0.01; \*\*\*P < 0.001.

## **Results**

### **Various formats of TRAIL**

We compared various formats of TRAIL: rhTRAIL, Fc-TRAIL, scTRAIL, and Fc-TRAIL. Figure 1 shows a schematic assembly of four different formats of TRAIL, including characteristics on their structure, in vivo pharmacokinetics, and in vitro cytotoxicity. Each protein was constructed as described in the materials and methods. Figure 1 illustrates the structure of various formats of TRAIL trimers and oligomerization. Figure 1 shows that rhTRAIL, Fc-TRAIL, scTRAIL, and Fc-scTRAIL exhibit terminal half-lives of 10 min, 100 min, 2.2 h, and 14.5 h, respectively. Fc-scTRAIL has the highest cytotoxic activity.

|                            | rhTRAIL   | Fc-TRAIL  | scTRAIL   | Fc-scTRAIL   |
|----------------------------|---|---|---|--|
| Peptide                    | TRAIL   | Fc TRAIL  | TRAIL TRAIL TRAIL   | Fc TRAIL TRAIL TRAIL   |
| Structure                  |  |  |  |           |
| Oligomerization            |   | Random oligomerization  |   | <br>Dimer |
| Half life                  | Less than 10 min  | 100 min   | 2.2 h   | 14.5 h   |
| EC <sub>50</sub> in HCT116 | 0.26 nM   |   | 1.1 nM  | 0.17 nM  |

**Figure 1:** Schematic assembly, structure, in vivo pharmacokinetics, and in vitro cytotoxicity of different formats of TRAIL proteins.

**Assessment of TRAIL in 3D culture**

To establish the 3D culture, 40 µl of Matrigel per well was used in a in 24-well plate. After trypsinization of SNU-1746 spheroids, 1x104 cells per well were mixed with Matrigel and then 40 µl of mixture per well was applied on the pre-warmed plates. After placing the plates in a 37°C, 5% CO2 incubator for complete polymerization, medium with was added to each well. Medium was changed in every two days and cells were treated with TRAIL 14 days after plating. To assess the cytotoxic effect of TRAIL in 3D culture, spheroids were treated with 1 nM rhTRAIL for various times and fluorescence images were analyzed. Figure 2A shows that significant PI staining was observed in 24 h-treated 3D cultures, but not 4 h-treated 3D cultures. Since DNA fragmentation is a hallmark of apoptosis, the PI staining data suggest that TRAIL-induced apoptosis can be detected 24 h after treatment in 3D culture, but not 4 h after treatment in 3D culture. Data from PI staining assay show that significant cytotoxicities occurred during treatment with 0.3 nM and 1 nM rhTRAIL for 24 h, but not at 4 h (Figure 2B). These observations were confirmed with PARP cleavage, a hallmark feature of apoptosis (Figure 2C).

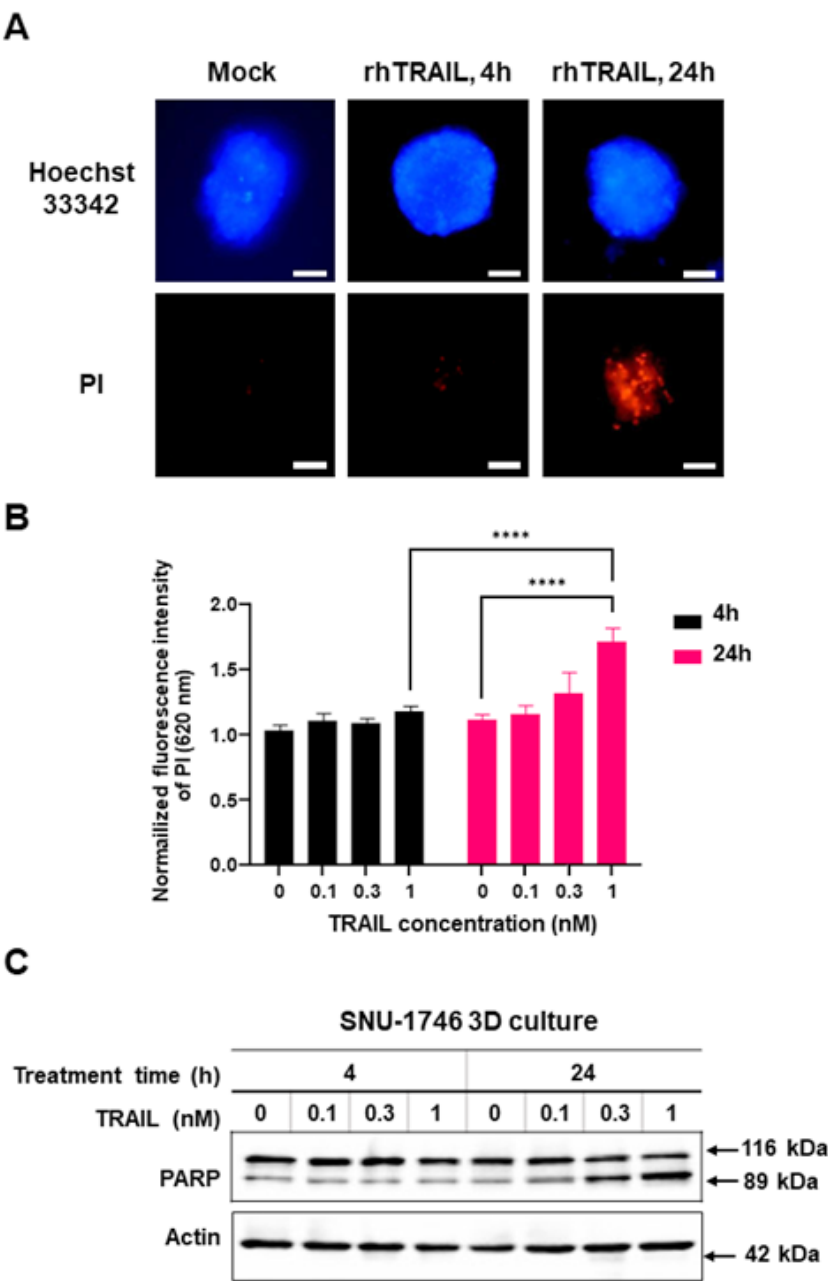


**Figure 2: Treatment of rhTRAIL into SNU-1746 spheroids.** SNU-1746 signet ring cells were grown as spheroids for 14 days in Matrigel and treated with rhTRAIL. (A) For fluorescence images, 1 nM rhTRAIL was treated into the spheroids for 4 h and 24 h and then the spheroids were stained with propidium iodide (PI) and Hoechst 33342. Representative images are shown, Scale bar: 30  $\mu$ m, (B) The spheroids were treated with various concentrations (0.1-1 nM) of rhTRAIL for 4 h or 24 h and stained with PI. Fluorescence intensity was measured and plotted. Error bars represent the mean  $\pm$  SD from triplicate experiments. For statistical analysis, one-way ANOVA was used. p-values: \*\*\*\*p < 0.001. (C) Whole-cell extracts were analyzed with immunoblotting assay using indicated antibodies. Actin was used to confirm equal amounts of proteins loaded in each lane.

Comparison of various types of TRAIL-induced apoptosis

Next, we further examined the effect of TRAIL by comparing various types of TRAIL. We employed four types of TRAIL: rhTRAIL, TRAIL consisting of only the biological active C-domain; Fc-TRAIL, immunoglobulin Fc domain fused TRAIL; scTRAIL, single chain TRAIL; and Fc-scTRAIL, immunoglobulin Fc domain fused single chain TRAIL. Data from immunoblotting assay and densitometry assay showed that PARP cleavage was detected in as low as 2 nM, 0.5 nM, 0.5 nM, and 0.1 nM for rhTRAIL, Fc-TRAIL, scTRAIL, and Fc-scTRAIL, respectively (Figure 3). These results illustrate that Fc-scTRAIL is the most efficient agent to induce apoptosis in 3D culture.

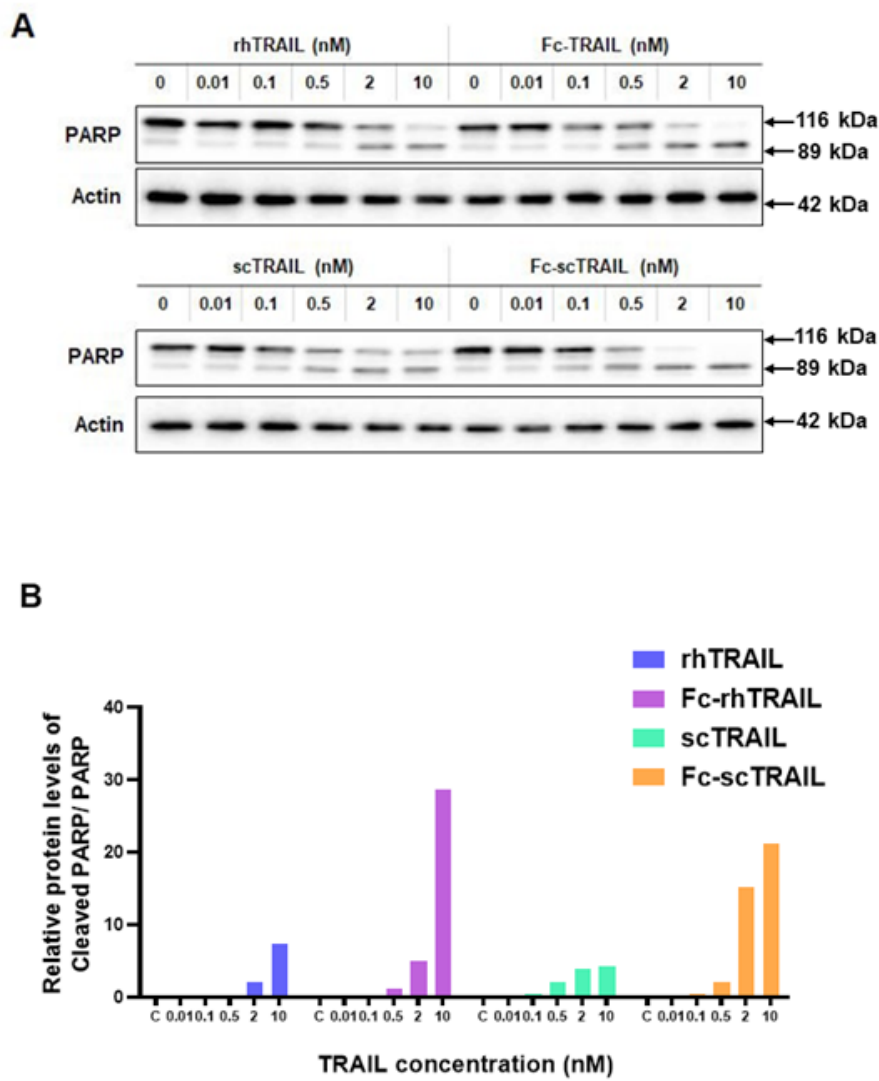
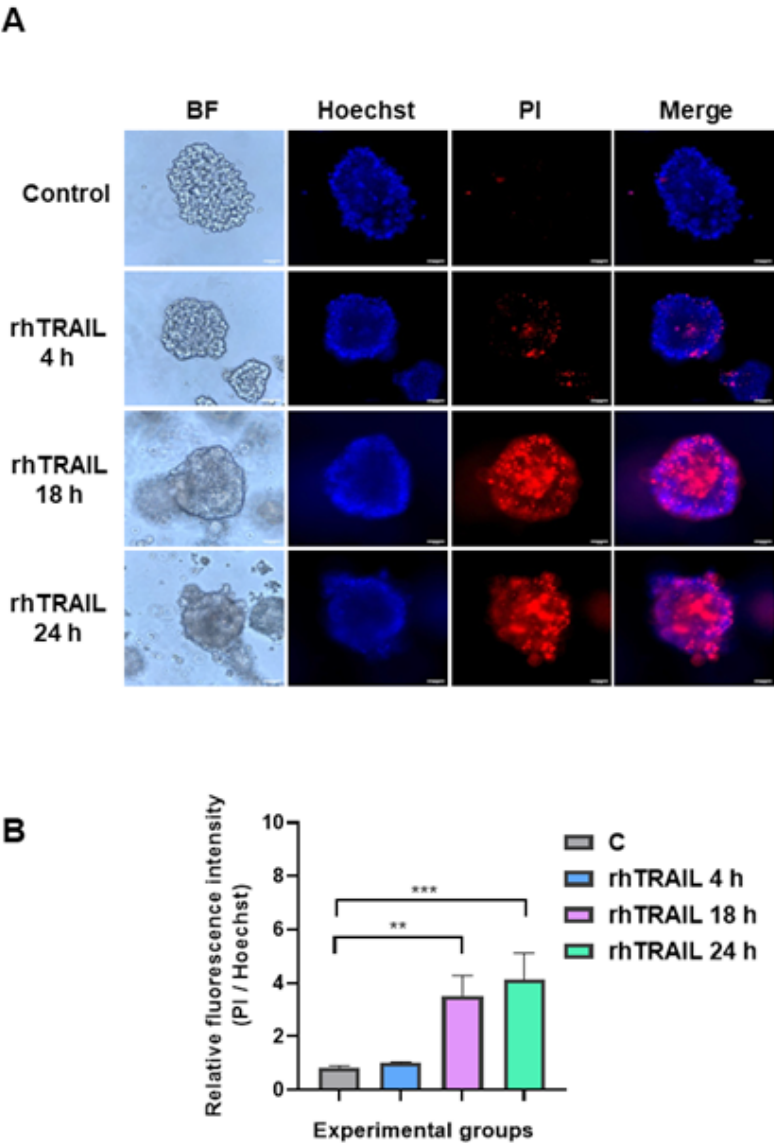


**Figure 3: Comparison of various types of TRAIL-induced apoptosis in SNU-1746 spheroids.** SNU-1746 signet ring cells were grown as spheroids for 14 days in Matrigel. The spheroids were treated with various concentrations of four different types of TRAILs, rhTRAIL, Fc-TRAIL, scTRAIL, and Fc-scTRAIL, for 24 h. (A) Whole-cell extracts were analyzed with immunoblotting assay using indicated antibodies. Actin was used to confirm equal amounts of proteins loaded in each lane. (B) Densitometry analysis of the bands from western blot was performed. Error bars represent the mean  $\pm$  SD from triplicate experiments.



**rhTRAIL and the ART/rhTRAIL combination induce apoptotic cell death in human colon tumoroids**

To extend our findings beyond conventional 3D cell cultures, we next assessed the cytotoxic effect of rhTRAIL in patient-derived colon tumoroids, which more closely display the structural complexity and cellular heterogeneity of solid tumors. As shown in Figure 4A, PI staining was significantly increased in tumoroids treated with rhTRAIL for 18 and 24 hours, while minimal staining was detected after 4 hours of treatment. Fluorescence intensity quantification confirmed that rhTRAIL induced significant cytotoxicity at 18 and 24 hours, but not at earlier time points (Figure 4B). Previous studies demonstrated that combination treatment with ferroptotic agents (ART, ERA) and TRAIL significantly enhances TRAIL-induced apoptosis in cancer cells [37, 39]. To determine whether ferroptotic agents promote TRAIL-induced apoptosis in a tumoroid model, we next examined the effect of combinatorial treatment (ART + rhTRAIL) on cytotoxicity at different time points. As shown in Figures 4C and 4D, data from the PI staining assay and quantitative analysis revealed that synergistic cytotoxicity was observed in tumoroids treated with ART in combination with rhTRAIL after 18 and 24 hours, whereas minimal staining was detected after 4 hours of treatment. These findings indicate that the ART/rhTRAIL combination induces time-dependent apoptosis in patient-derived tumoroids.



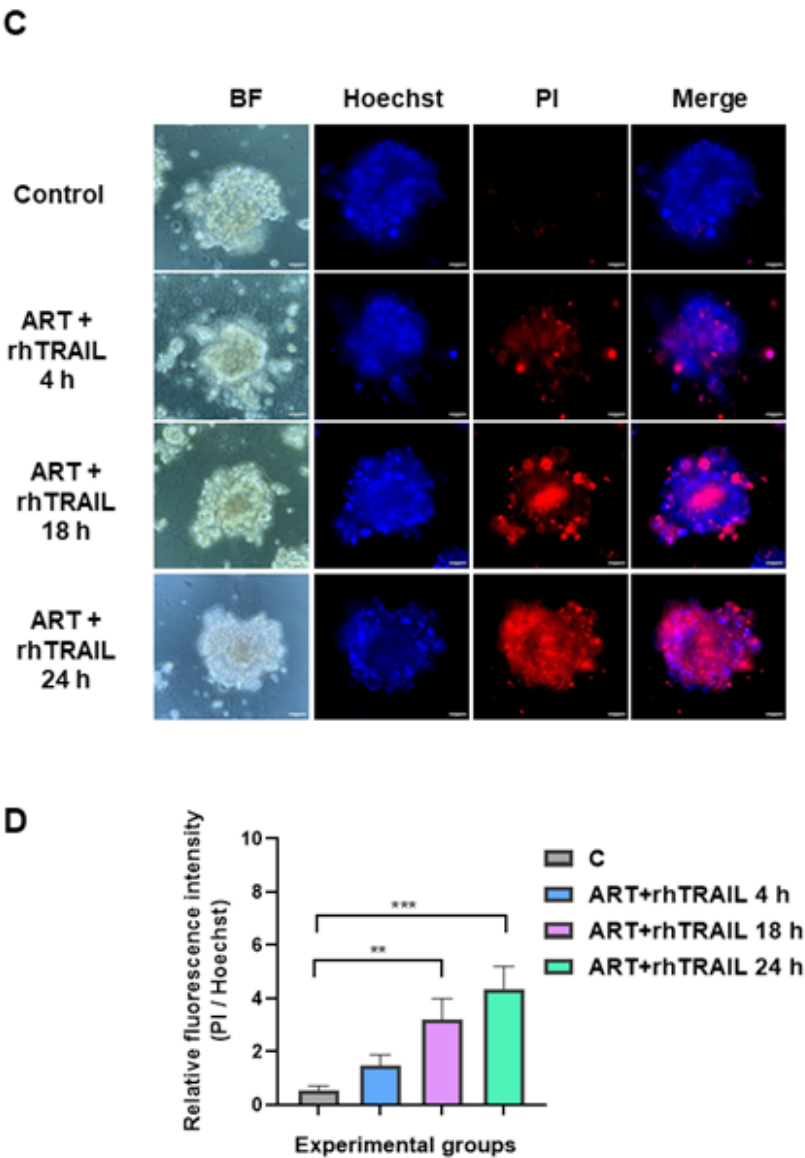


**Figure 4: Assessment of rhTRAIL only or combined ART and rhTRAIL-induced cytotoxicity in human colon tumoroids.** Tumoroids were incubated in the absence or presence of rhTRAIL (2.5 nM) for various times (4-24 h) and then stained with 50 µg/mL propidium iodide (PI) to detect non-viable cells. Nuclei were counterstained with Hoechst to visualize total cell populations. (A) Morphological features were analyzed using an ECHO Revolve microscope. BF, bright field. Representative images are shown (scale bar: 200 µm). (B) Fluorescence intensity was measured and plotted. Error bars represent the mean ± SD from triplicate experiments. For statistical analysis, one-way ANOVA was used. p-values: \*\*p < 0.01; \*\*\*p < 0.001. (C) Tumoroids were pretreated with ART (50 µM) for 20 h and then exposed to rhTRAIL (2.5 nM) for various times (4-24 h), followed by staining with 50 µg/mL PI. Nuclei were counterstained with Hoechst (1:2000 in PBS). Morphological features were analyzed using an ECHO Revolve microscope. BF, bright field. Representative images are shown (scale bar: 200 µm). (D) Fluorescence intensity was measured and plotted. Error bars represent the mean ± SD from triplicate experiments. For statistical analysis, one-way ANOVA was used. p-values: \*\*p < 0.01; \*\*\*p < 0.001.

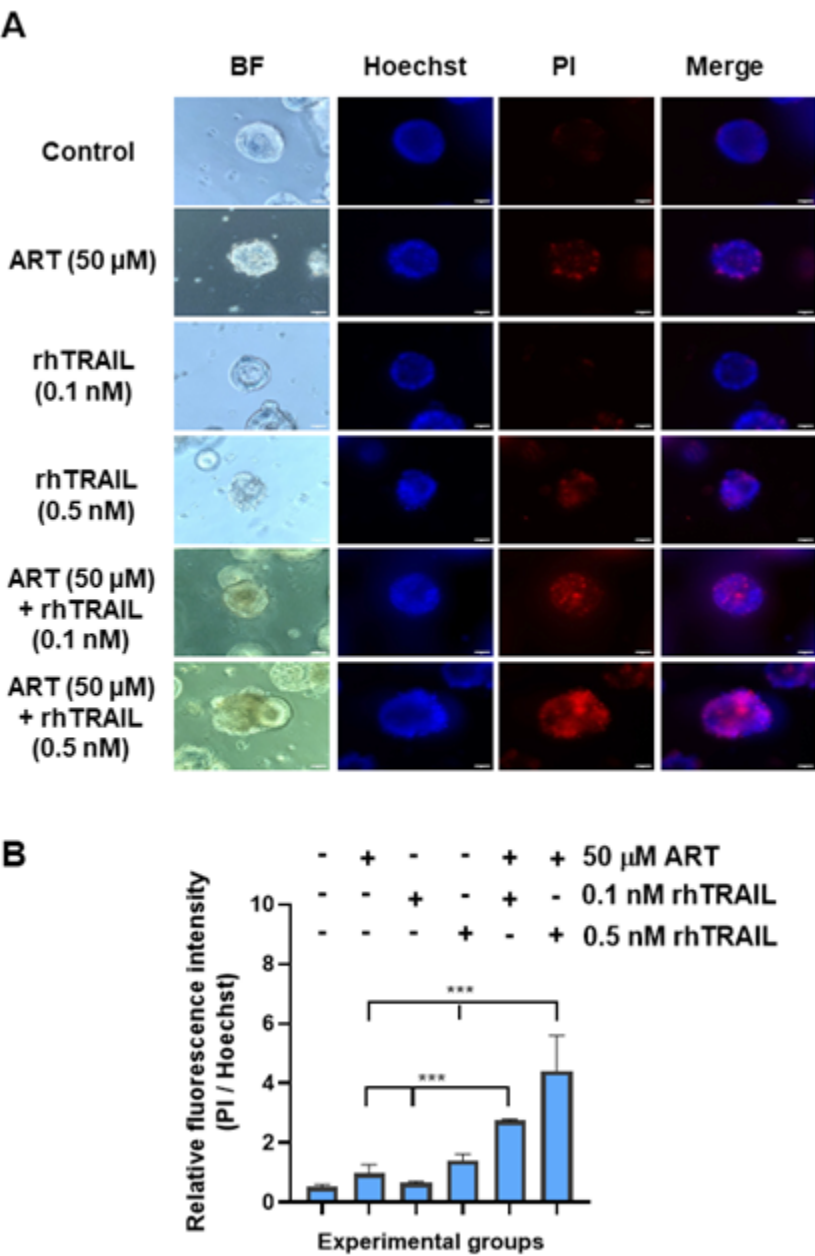
**ART enhances rhTRAIL-induced apoptosis and mitochondrial membrane potential alteration in human colon tumoroids**

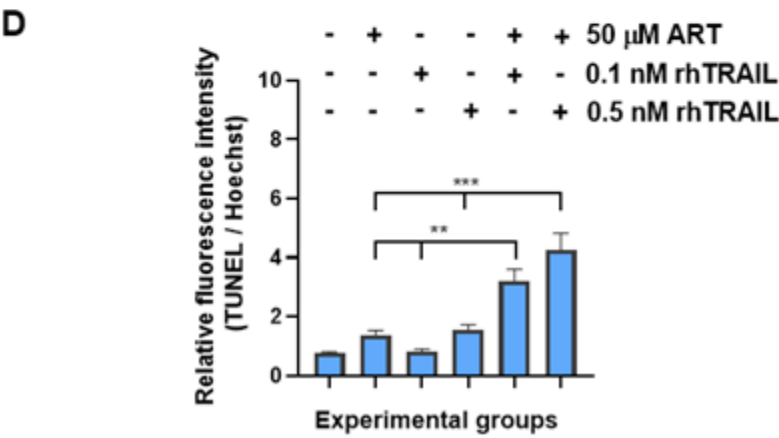
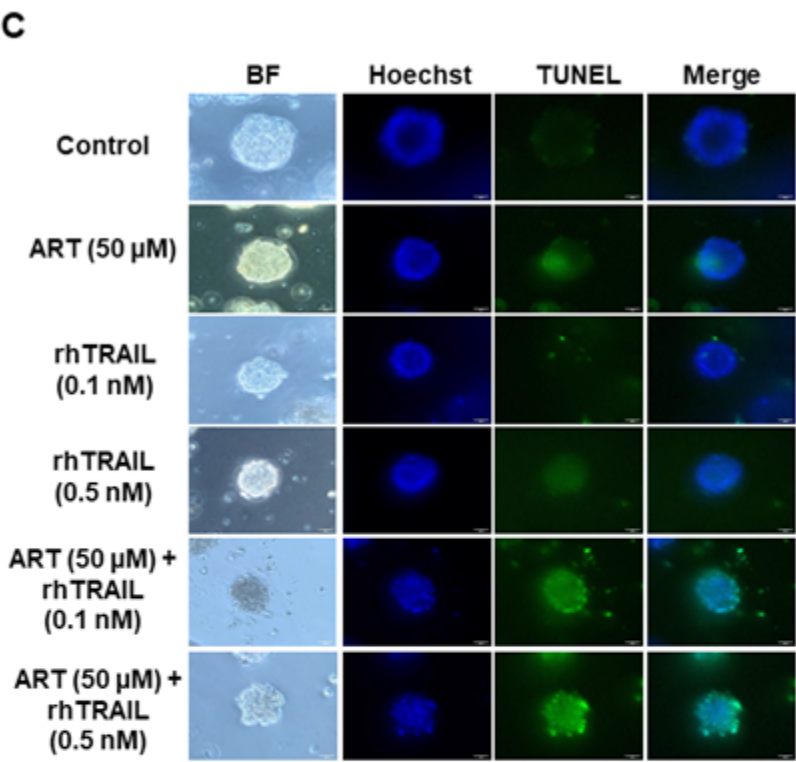
Since our previous results demonstrated that the combination of ART and rhTRAIL induced significant apoptosis after 24 hours after treatment in tumoroids, we next examined the synergistic effect of combinatorial treatment (ART + rhTRAIL) with different concentrations of rhTRAIL (0.1, 0.5 nM) in tumoroids. As shown in Figure 5A, a synergistic effect was observed with combination treatments, particularly the combination of ART with 5 nM rhTRAIL, while cell death was only slightly induced in response to single treatments. Moreover, quantitative analysis of fluorescence intensity confirmed a significant increase in apoptotic cell death following combination treatment compared to rhTRAIL alone (Figure 5B). Combination index analysis revealed a strong synergy of ART and rhTRAIL treatment (Table 1). A combination of ART with various concentrations of rhTRAIL, either 0.1 or 0.5 nM, induced a strong synergistic effect. To further assess apoptosis induction, we performed the TUNEL assay to quantify apoptosis during treatment with ART and rhTRAIL (Figure 5C). Data from fluorescent imaging showed that the combined treatment resulted in significantly higher DNA fragmentation in TUNEL-positive staining compared to the single treatments (Figure 5C). Quantitative analysis indicated a substantial increase in DNA fragmentation following ART/rhTRAIL combination treatment (Figure 5D). Furthermore, the effect of the ART and rhTRAIL combination on mitochondrial membrane potential was examined using JC-1 staining. In control cells (non-apoptotic cells), JC-1 accumulates as aggregates with red fluorescence, indicative of intact mitochondrial membrane potential. In comparison, the combined treatment of ART and rhTRAIL showed a shift toward green fluorescence, suggesting a loss of mitochondrial membrane potential (Figure 5E). These findings indicate that ART significantly enhances rhTRAIL-induced apoptosis and mitochondrial membrane depolarization in tumoroids.

| rhTRAIL (nM) | Fc-TRAIL (nM) | Fc-scTRAIL (nM) | ART (µM) | CI Value    |
|--------------|---------------|-----------------|----------|-------------|
| 0.1          | -             | -               | 50       | 0.27171#### |
| 0.5          | -             | -               | 50       | 0.05389###  |
| -            | 0.1           | -               | 50       | 0.05342#### |
| -            | 0.5           | -               | 50       | 0.02770###  |
| -            | -             | 0.1             | 50       | 0.25749#### |
| -            | -             | 0.5             | 50       | 0.17875#### |

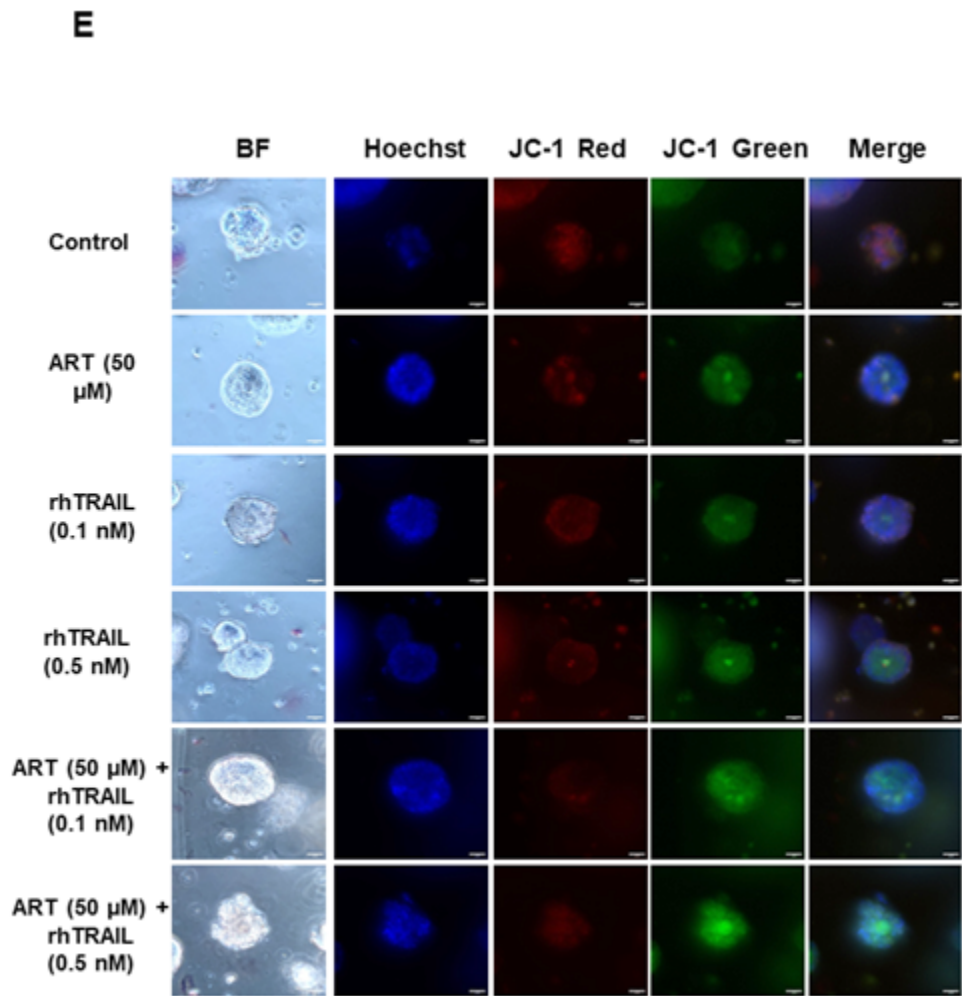
0.9-1.10: additive effect, #: slight synergy; ##: moderate synergy; ####: strong synergy

**Table 1:** Combination index (CI).





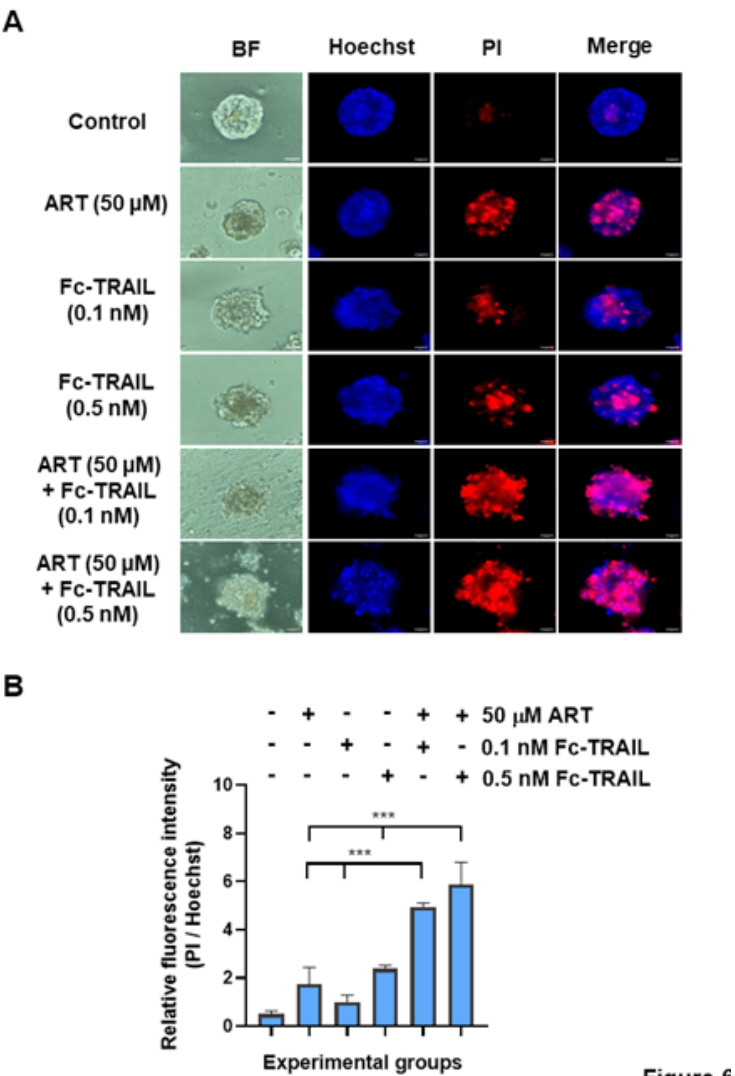


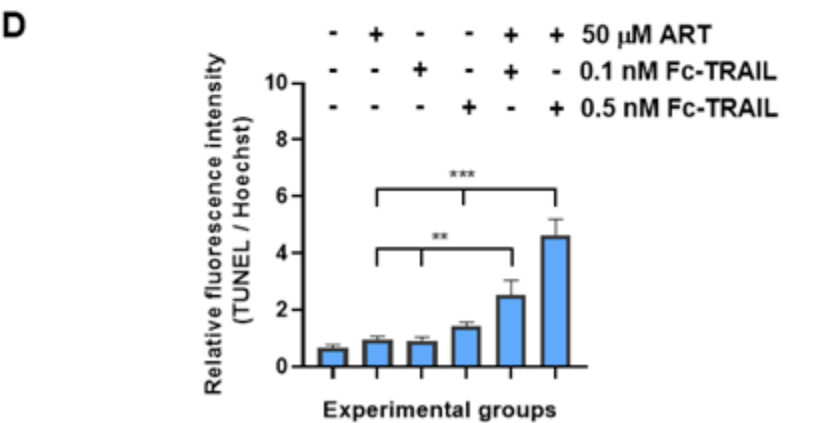
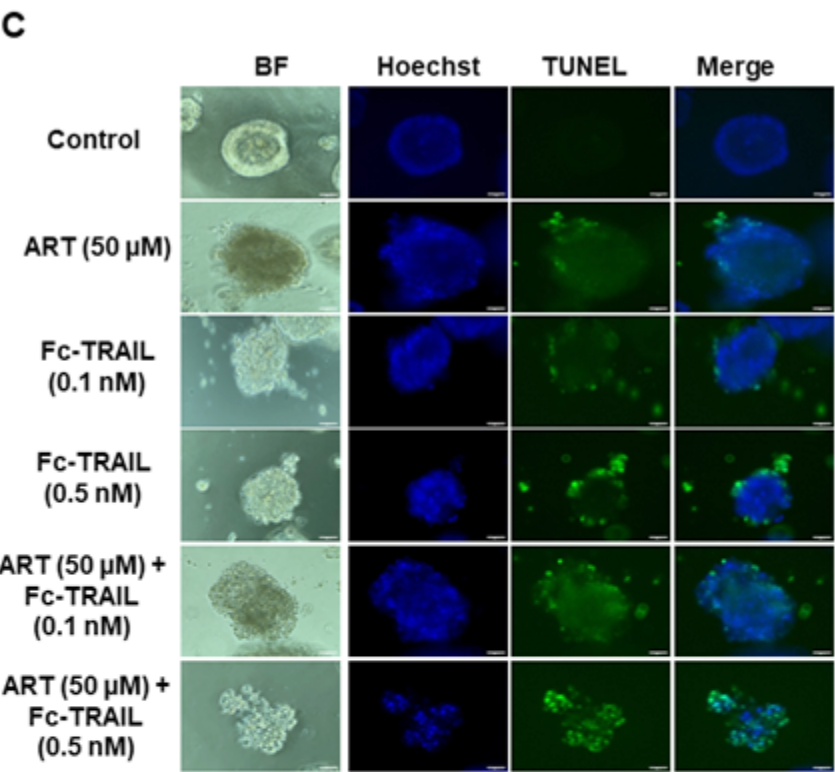


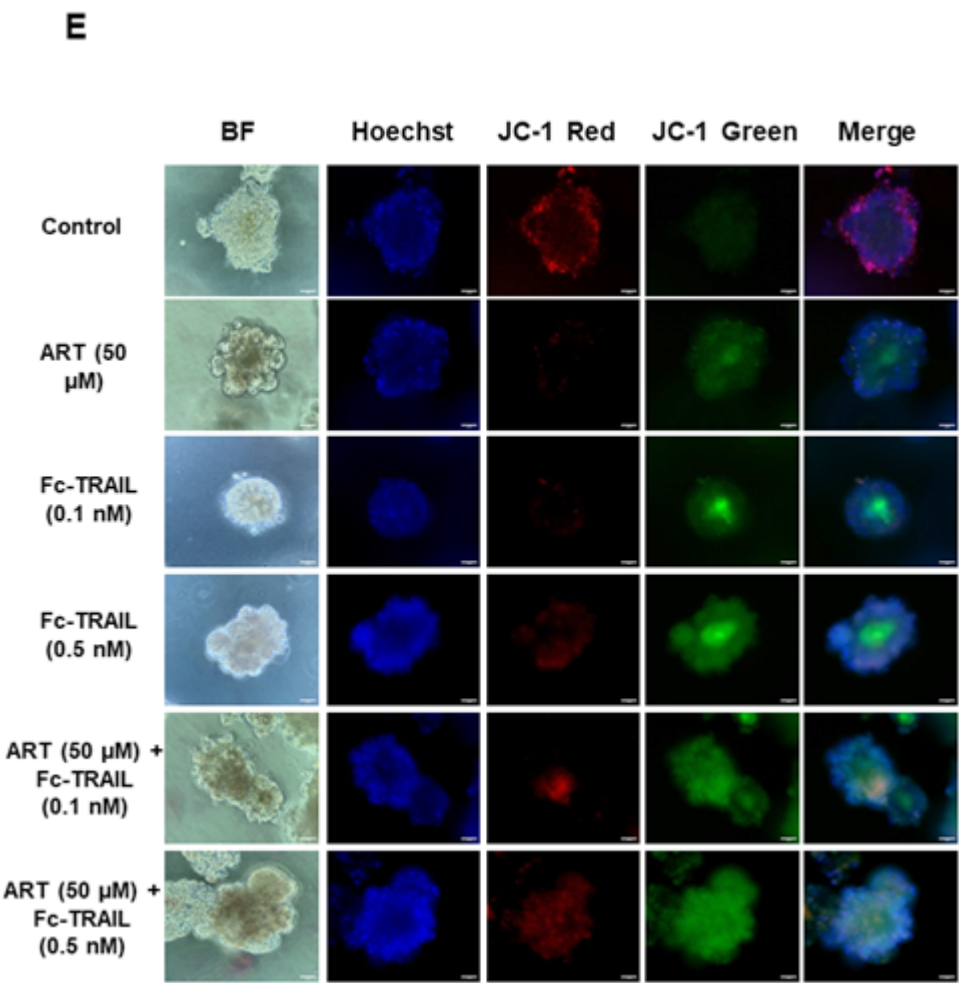
**Figure 5: ART promotes rhTRAIL-induced apoptosis and alteration in mitochondrial membrane potential in human colon tumoroids.** Tumoroids were pretreated with ART (50 μM) for 20 h and then incubated with various concentrations of rhTRAIL (0.1, 0.5 nM) for 24 h followed by staining with 50 μg/mL propidium iodide (PI) and Hoechst (1:2000 in PBS). (A) Morphological features were analyzed using an ECHO Revolve microscope. BF, bright field. Representative images are shown (scale bar: 200 μm). (B) Fluorescence intensity was measured and plotted. Error bars represent the mean ± SD from triplicate experiments. For statistical analysis, one-way ANOVA was used. p-values: \*\*\*p < 0.001. (C) TUNEL staining assay was performed, and fluorescent images were examined using an ECHO fluorescence microscope. Representative images are shown (scale bar: 200 μm). (D) Fluorescence intensity was measured and plotted. Error bars represent the mean ± SD from triplicate experiments. For statistical analysis, one-way ANOVA was used. p-values: \*\*p < 0.01; \*\*\*p < 0.001. (E) Tumoroids were stained with JC-1 dye, and JC-1 fluorescence mitochondrial images were examined using an ECHO fluorescence microscope.

**ART promotes Fc-TRAIL-induced apoptosis and mitochondrial membrane potential alteration in human colon tumoroids**

Fc-TRAIL is known as a more effective apoptosis-inducing agent compared to rhTRAIL, as our initial experiments in 3D culture revealed that Fc-TRAIL exhibits stronger pro-apoptotic effects compared to rhTRAIL. We next tested whether combination treatment of ART and Fc-TRAIL could effectively enhance apoptosis induction in tumoroids. Data from the PI staining assay demonstrated that a synergistic effect was observed with the combination treatments, particularly with ART plus 5 nM Fc-TRAIL, while cell death was only slightly induced in response to single treatments (Figure 6A). The results were also supported by quantitative analysis of fluorescence intensity (Figure 6B). Combination index analysis indicated a strong synergy of ART and Fc-TRAIL treatment (Table 1). A combination of ART with various concentrations of Fc-TRAIL, either 0.1 or 0.5 nM, induced a strong synergy. To quantify DNA fragmentation during combination treatment of ART and Fc-TRAIL, we performed a TUNEL assay, which showed significantly higher DNA fragmentation in the combined treatments compared to single treatments (Figure 6C). Similar results were obtained by quantitative analysis, which indicated a remarkable increase in DNA fragmentation following combined treatment, as shown in Figure 6D. Moreover, mitochondrial membrane potential changes were assessed using JC-1 staining. As shown in Figure 6E, in control cells, JC-1 forms aggregates resulting in red fluorescence, indicative of intact mitochondrial membrane potential, while tumoroids treated specifically with the ART and Fc-TRAIL combination showed a shift toward green fluorescence, suggesting a loss of mitochondrial membrane potential. These results demonstrate that ART significantly enhances Fc-TRAIL-induced apoptosis and mitochondrial membrane depolarization in tumoroids.



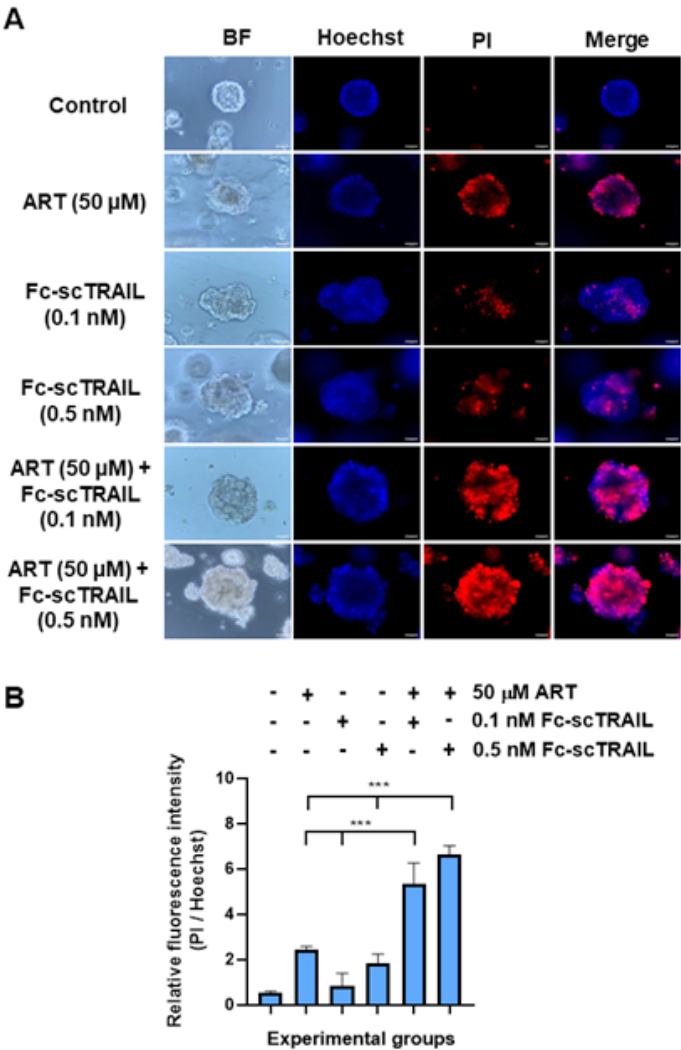




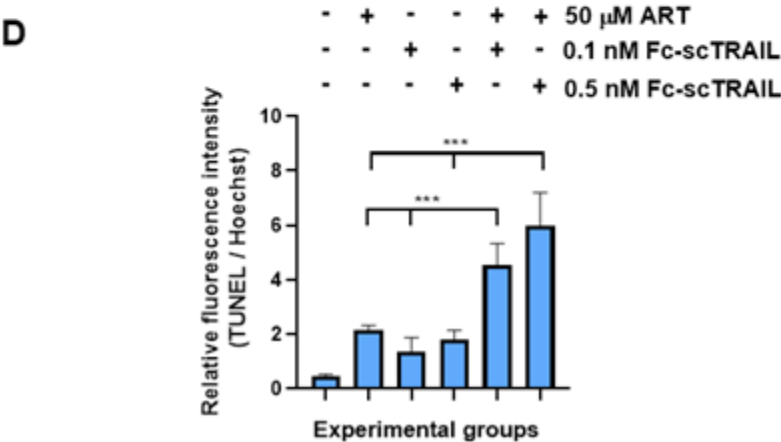
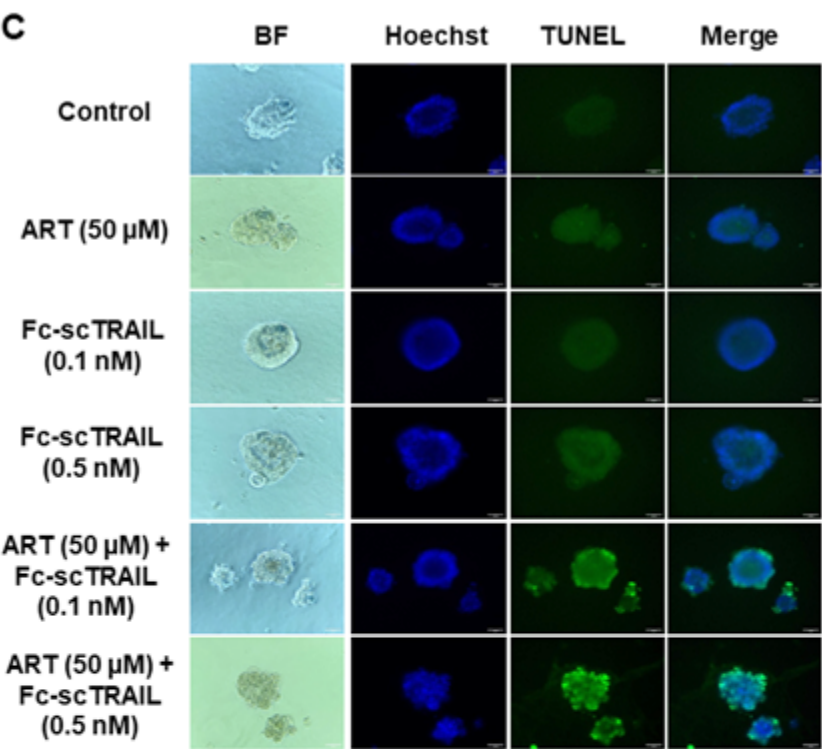
**Figure 6: Assessment of combined ART and Fc-TRAIL-induced cytotoxicity, apoptosis, and mitochondrial membrane potential change in human colon tumoroids.** Tumoroids were pretreated with ART (50 μM) for 20 h and then exposed to various concentrations of Fc-TRAIL (0.1, 0.5 nM) for an additional 24 h followed by staining with 50 μg/mL propidium iodide (PI) and Hoechst (1:2000 in PBS). (A) Morphological features were examined using an ECHO Revolve microscope. BF, bright field. Representative images are shown (scale bar: 200 μm). (B) Fluorescence intensity was measured and plotted. Error bars represent the mean ± SD from triplicate experiments. For statistical analysis, one-way ANOVA was used. p-values: \*\*\*p < 0.001. (C) TUNEL staining assay was performed, and fluorescent images were captured using an ECHO fluorescence microscope. Representative images are shown (scale bar: 200 μm). (D) Fluorescence intensity was measured and plotted. Error bars represent the mean ± SD from triplicate experiments. For statistical analysis, one-way ANOVA was used. p-values: \*\*p < 0.01; \*\*\*p < 0.001. (E) Tumoroids were stained with JC-1 dye, and mitochondrial fluorescence images were obtained using an ECHO fluorescence microscope.

**ART promotes Fc-scTRAIL-induced apoptosis and mitochondrial membrane potential alteration in human colon tumoroids**

Since our previous results indicated that Fc-scTRAIL induced apoptosis significantly in 3D culture, we next examined the induction of cell death in the tumoroid model in response to ART with Fc-scTRAIL combination treatment. As shown in Figure 7A, a significant effect was observed with combination treatments, particularly the combination of ART with 5 nM Fc-scTRAIL, whereas cell death induction was only slightly induced in response to single treatments. Furthermore, quantitative analysis of fluorescence intensity confirmed a significant increase in apoptotic cell death following combination treatment compared to Fc-scTRAIL alone (Figure 7B). Combination index analysis revealed a strong synergy of ART and Fc-scTRAIL treatment (Table 1). A combination of ART with various concentrations of Fc-scTRAIL, either 0.1 or 0.5 nM, induced a strong synergy. To further validate the induction of apoptosis, we performed the TUNEL assay to quantify apoptosis during treatment with ART and Fc-scTRAIL (Figure 7C). Data from fluorescent imaging showed that the combined treatment resulted in significantly higher DNA fragmentation in TUNEL-positive staining compared to the single treatments (Figure 7C). Similar results were obtained by quantitative analysis, which indicated a remarkable increase in DNA fragmentation following combined treatment, as shown in Figure 7D. Additionally, the effect of the ART and Fc-scTRAIL combination on mitochondrial membrane potential was assessed using JC-1 staining. As shown in Figure 7E, in control cells (non-apoptotic cells), JC-1 accumulates as aggregates with red fluorescence, indicative of intact mitochondrial membrane potential, whereas combined treatment with ART and Fc-scTRAIL showed a shift toward green fluorescence, suggesting a loss of mitochondrial membrane potential. These findings indicate that ART significantly augments Fc-scTRAIL-induced apoptosis and mitochondrial membrane depolarization in tumoroids.







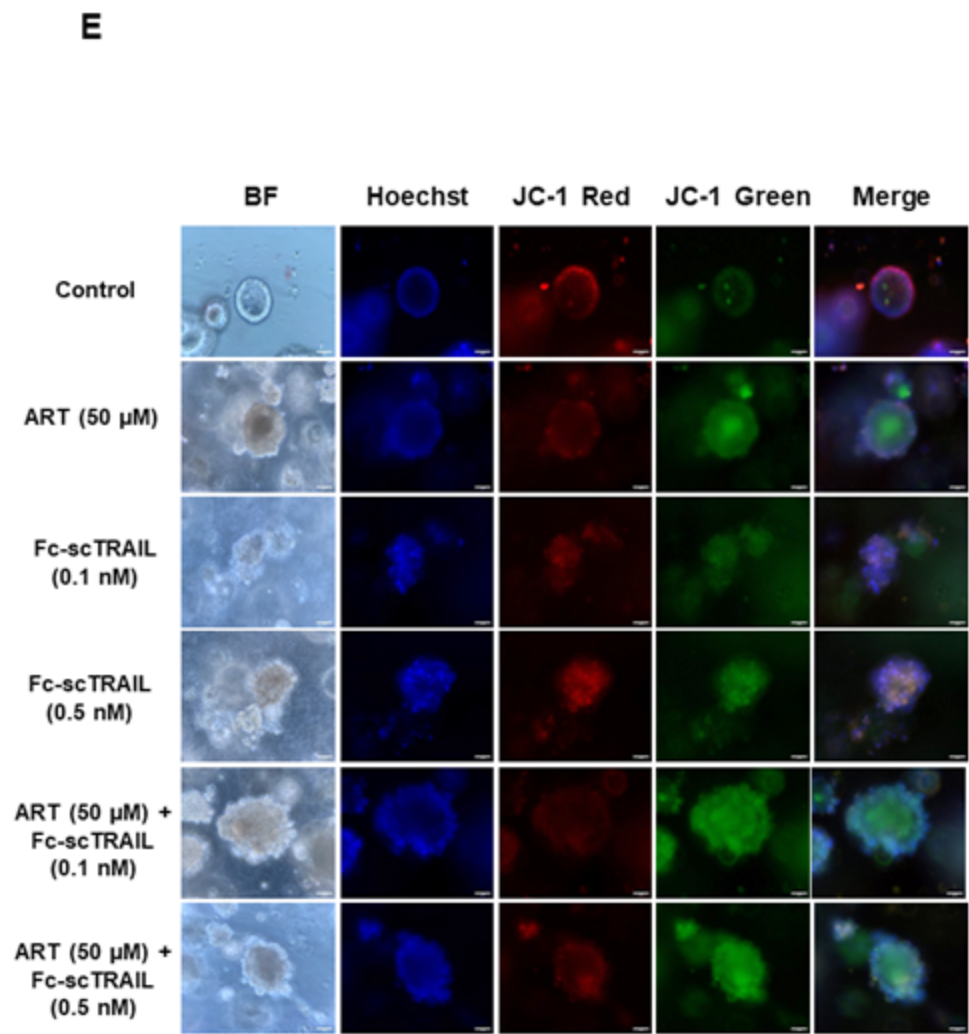


**Figure 7: Assessment of combined ART and Fc-scTRAIL-induced cytotoxicity, apoptosis, and mitochondrial membrane potential change in human colon tumoroids.** Tumoroids were pretreated with ART (50 μM) for 20 h, with or without Fc-scTRAIL (0.1, 0.5 nM) for an additional 24 h followed by staining with 50 μg/mL propidium iodide (PI) and Hoechst (1:2000 in PBS). (A) Morphological changes were assessed using an ECHO Revolve microscope. BF, bright field. Representative images are shown (scale bar: 200 μm). (B) Fluorescence intensity was quantified and plotted. Error bars represent the mean ± SD from triplicate experiments. Statistical analysis was performed using one-way ANOVA. p-values: \*\*\*p < 0.001. (C) TUNEL staining was conducted, and fluorescent images were obtained using an ECHO fluorescence microscope. Representative images are shown (scale bar: 200 μm). (D) Fluorescence intensity was quantified and plotted. Error bars represent the mean ± SD from triplicate experiments. Statistical analysis was performed using one-way ANOVA. p-values: \*\*\*p < 0.001. (E) Tumoroids were stained with JC-1 dye, and mitochondrial fluorescence images were obtained using an ECHO fluorescence microscope.

**Comparison of various types of TRAIL-induced apoptosis in human colon tumoroids**

After analyzing different TRAIL formats, alone or in combination with ART in tumoroids, we performed a comparative analysis of all three TRAIL formats by immunoblotting. As shown in Figures 8A, 8B, and 8C, whole-cell extracts were analyzed by immunoblotting using the indicated antibodies. Actin was used as a loading control to confirm equal protein amounts in each lane. The protein expression levels of the apoptotic marker PARP cleavage showed a concentration-dependent increase in apoptosis induction, particularly in response to ART + Fc-scTRAIL. The results revealed that treatment with rhTRAIL led to minimal changes in apoptotic marker levels, while Fc-TRAIL induced apoptosis to a lesser extent than Fc-scTRAIL (Figure 8A–C).. These results demonstrate that the Fc-scTRAIL format is the most effective apoptosis inducer when combined with ART in human colon tumoroids.

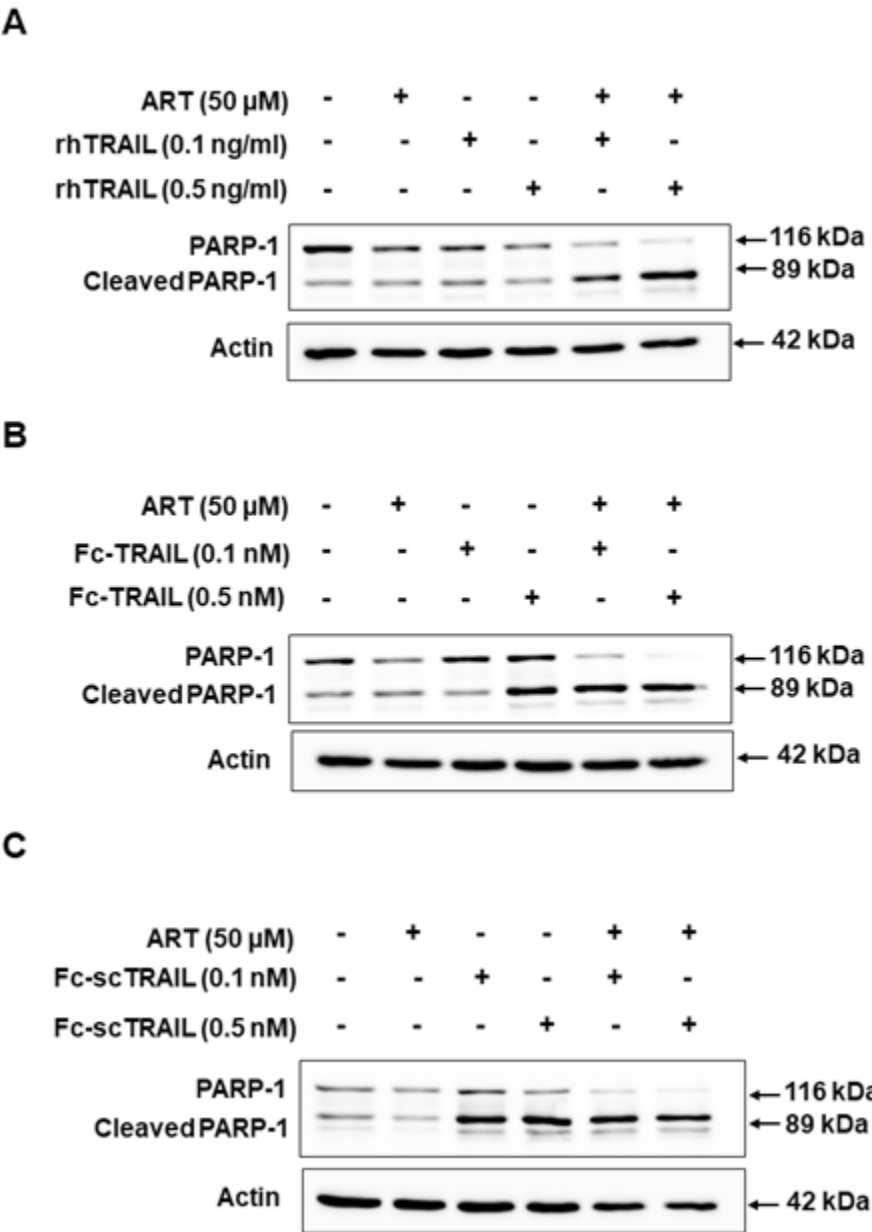


**Figure 8: Comparison of different formats of TRAIL-induced apoptosis in human colon tumoroids.** Tumoroids were pretreated with ART (50  $\mu$ M), followed by incubation with various concentrations (0.1, 0.5 nM) of three different TRAIL formats: rhTRAIL, Fc-TRAIL, and Fc-scTRAIL, for 24 h. (A–C) Whole-cell extracts were analyzed by immunoblotting using the indicated antibodies. Actin was used as a loading control to confirm equal protein amounts in each lane.

## Discussion

In this study, we compared the apoptotic activity of four different types of TRAIL in 3D cell cultures. Unlike 2D monolayer cultures, 3D spheroid and tumoroid cultures require a longer rhTRAIL treatment time to induce apoptosis. Moreover, the dimeric Fc-scTRAIL fusion protein is the most efficient agent among the various TRAIL formats for inducing apoptosis in 3D spheroid and tumoroid cultures. Additionally, we observed that combining TRAIL agents with the ferroptotic agent artesunate (ART) markedly enhances apoptosis induction, particularly when Fc-scTRAIL is combined with ART in tumoroids.

Previous studies demonstrate that morphological (membrane blebbing) and biochemical (PARP-1 cleavage) features of apoptosis can be detected via microscopy and polyacrylamide gel electrophoresis, respectively. We previously observed that apoptosis was detected as early as 2 h post-treatment with rhTRAIL in 2D cultures of cancer cells and it took 4–6 h to induce maximum apoptosis [40]. Unlike 2D cultures, it takes longer to induce apoptosis when 3D cell spheroid and tumoroid cultures are treated with rhTRAIL. This is probably due to the limitation of rhTRAIL penetration and distribution in 3D culture. Since 3D multicellular layer cultures recapitulate barriers to this limitation, data with 3D culture better represent the composition of a tumor in the body than cancer cell lines.

In this study, we compared the apoptotic activity of four different types of TRAIL. Even though all exhibit trimer complex formation, the activity of TRAIL can be improved by constructing dimeric immunoglobulin fused TRAIL, in particular scTRAIL (Figure 1). Dimeric Fc-scTRAIL fusion proteins increases the valency of scTRAIL and their in vivo half-lives by utilizing an additional  $\gamma$ Fc region as a dimerization module [27, 26]. Moreover, targeted dimeric single-chain fragment variable immunoglobulin Fc domain-fused single chain TRAIL (scFv-Fc-scTRAIL) fusion proteins directed against various tumor-associated antigens (TAAs) have been shown to exert considerably higher activity compared with unmodified TRAIL [16]. We will employ antibody moieties directed against TAAs such as epidermal growth factor receptor (EGFR), c-mesenchymal epithelial transition factor (c-MET), tyrosine-protein kinase Kit (c-KIT), and platelet-derived growth factor receptor alpha (PDGFRA), which are overexpressed

in tumor tissues [41] and evaluate the superior properties of Fc-comprising scTRAIL fusion proteins in 3D cell spheroid cultures in the near future.

To better reflect the physiological characteristics of solid tumors, we extended patient-derived colon tumoroids into our study. In contrast to established cancer cell lines, tumoroids retain the key features of primary tumors, including tissue architecture and the genetic heterogeneity of the original tumors, making them particularly valuable for preclinical drug screening [42]. Our data show that rhTRAIL induces a time-dependent increase in apoptotic cell death in tumoroids, with substantial apoptotic responses observed only after 18–24 hours of treatment (Figure 4). These observations are consistent with prior reports, which propose that the restricted diffusion and slow penetration of therapeutic agents in compact 3D structures slow down apoptotic responses [43]. Our findings demonstrate that ART substantially enhances rhTRAIL-induced apoptosis in patient-derived colon tumoroids, supporting its role as a TRAIL sensitizer. The observed synergy suggests that ART may overcome the resistance typically seen in 3D tumor models by inducing mitochondrial dysfunction and activating intrinsic apoptotic pathways. This is consistent with earlier reports showing that ART can downregulate anti-apoptotic proteins and increase oxidative stress, thereby contributing to apoptosis [44]. Enhanced DNA fragmentation and mitochondrial depolarization further support the involvement of the intrinsic apoptotic pathway. As resistance to TRAIL is frequently linked to mitochondrial dysfunction and survival signaling [45], combining ART with rhTRAIL may represent an effective strategy to overcome apoptosis resistance in colorectal cancer.

We observed that the effectiveness of ART augmentation differed in different TRAIL formats. Fc-TRAIL and Fc-scTRAIL, known for its higher apoptotic efficiency compared to rhTRAIL due to enhanced molecular stability and bivalent configuration, showed effectively augmented antitumor efficacy when paired with ART in tumoroid models (Figure 6). This combination led to a significant increase in apoptosis, evidenced by enhanced nuclear fragmentation, elevated DNA damage, and mitochondrial membrane depolarization. These results are consistent with previous reports demonstrating that Fc-fused TRAIL formats exhibit improved pharmacokinetic properties and more efficient tumor-specific engagement [24]. Similar synergistic effects were observed with the combination of ART and Fc-scTRAIL, which demonstrated the strongest pro-apoptotic response among all tested treatment groups in human colon tumoroids (Figure 7). This combination resulted in extensive nuclear condensation, marked DNA fragmentation, and a pronounced loss of mitochondrial membrane potential, indicating substantial activation of both intrinsic and extrinsic apoptotic signaling pathways. Fc-scTRAIL, a fusion protein combining the trimeric TRAIL ligand with an Fc domain, provides prolonged

serum half-life, forms stable and higher-order multimeric structures, and enhanced receptor clustering ability—features that increase its apoptotic potency compared to monomeric or dimeric TRAIL formats [26, 24]. Furthermore, the addition of ART appears to markedly amplify these effects by lowering the apoptotic threshold through mechanisms involving the induction of ferroptosis-associated oxidative stress [46]. These findings highlight the promise of co-activating ferroptotic and apoptotic pathways as a strategy to overcome resistance and elicit stronger anti-tumor effects in tumoroid cancer models.

## Conclusion

In conclusion, our findings demonstrate that various TRAIL formats exhibit different efficacies in 3D spheroids as well as tumoroids. The results from these studies suggest that these cultures require longer rhTRAIL treatments, likely due to slower penetration in the multicellular layer. We also observed that Fc-scTRAIL exhibits the highest apoptotic activity, likely due to the increased valency of scTRAIL through dimerization. Furthermore, we demonstrate that combining the ferroptotic agent ART with various TRAIL formats significantly enhances apoptosis in human CRC tumoroids. Combined treatment with ART and TRAIL formats resulted in increased apoptotic cell death, enhanced DNA fragmentation, and mitochondrial membrane depolarization, with Fc-scTRAIL showing the most robust apoptotic response. These findings were supported by combination index analyses and elevated PARP cleavage. Taken together, our results highlight Fc-scTRAIL, especially in combination with ferroptosis inducers, as a promising strategy to promote apoptosis in complex tumor models. Future research will focus on optimizing targeted constructs and evaluating their in vivo efficacy.

## Acknowledgements

We thank Lila Mouakkad (Department of Biomedical Sciences, Cedars-Sinai Medical Center) for her critical review of the manuscript. We thank Professor Xiangwei Wu (University of Texas MD Anderson Cancer Center, Houston, TX, USA) for kindly providing Fc-TRAIL plasmid. This work was supported by the following grants: National Institutes of Health R21CA259243 and R01CA265827, and Department of Defense W81XWH-22-1-1095 RA210084.

**Ethical Approval:** Ethical approval for this study was approved by Cedar-Sinai's Institutional Review Board (STUDY 00002365).

**Conflicts of Interest:** The authors declare that they have no conflicts of interest.

**Availability of data and materials:** Research materials that were generated in the studies including plasmid DNA constructs will be made freely available to the scientific research community as soon

as this manuscript has been documented in a publication. Raw data were generated at the Cedars-Sinai Medical Center. Derived data supporting the findings of this study are available from the corresponding author Dr. Yong J. Lee on request.

**Author Contributions:** F.V. and S.H. collected the data. A.G., J-L.K. and R.K. provided materials. F.V., S.H., and YJ L. participated in analyzing data and interpretation. F.V. and Y.J.L. drafted the manuscript. All authors read and approved the final manuscript.

**Grant Sponsor:** National Cancer Institute R21 CA259243 (Y.J.L.), National Cancer Institute R01 CA265827 (Y.J.L.), Department of Defense OC190038 (W81XWH-20-1-0190) (Y.J.L.), Department of Defense RA210084 (W81XWH-22-1-1095) (Y.J.L.)

**Data Availability Statement:** Data sources will be made freely available to the scientific research community from the corresponding author upon reasonable request as soon as they have been documented in a publication.

## Abbreviations Used in This Paper:

2D-two dimensional;  
3D-three dimensional;  
APO2L-apoptosis ligand 2;  
ART-Artesunate;  
Bak-BCL2 Antagonist/Killer;  
Bax-BCL2 Associated X;  
Bid-BH3 interacting-domain death agonist;  
DcR1-decoy receptor 1;  
DcR2-decoy receptor 2;  
DISC-death-inducing signaling protein complex;  
DR-death receptor;  
DD-death domain; DR4, death receptor 4;  
DR5-death receptor 5;  
EGFR-Epidermal growth factor receptor;  
FADD-Fas-associated death domain;  
FasL-Fas ligand;  
Fc-scTRAIL-immunoglobulin Fc domain-fused single-chain version of TRAIL;  
Fc-TRAI- immunoglobulin Fc domain-fused TRAIL;  
FLAG- DYKDDDDK Peptide;



His-tagged-polyhistidine-tagged;  
 HRP- horseradish peroxidase;  
 c-KIT-tyrosine-protein kinase Kit;  
 c-MET-c-mesenchymal epithelial transition factor;  
 PARP- poly (ADP-ribose) polymerase;  
 PDGFRA-platelet-derived growth factor receptor alpha;  
 PI- propidium iodide;  
 rhTRAIL- recombinant human TRAIL;  
 scFv-single-chain fragment variable;  
 SD- standard deviation;  
 tBid-truncated Bid;  
 TAA-tumor-associated antigens;  
 TNF- tumor necrosis factor;  
 TRAIL- tumor necrosis factor-related apoptosis-inducing ligand;  
 TRAIL-R1- tumor necrosis factor-related apoptosis inducing ligand receptor 1;  
 TRAIL-R2- tumor necrosis factor-related apoptosis inducing ligand receptor 2.

## References

- Vafaieinik F, Zhang L, Lee YJ (2025) Low extracellular pH enhances TRAIL-induced apoptosis by downregulating Mcl-1 expression. *Exp Cell Res* 447:114481.
- Xiang L, He B, Liu Q, Hu D, Liao W, et al. (2020) Antitumor effects of curcumin on the proliferation, migration and apoptosis of human colorectal carcinoma HCT116 cells. *Oncol Rep* 44:1997-2008.
- Yangnok K, Innajak S, Sawasjirakij R, Mahabusarakam W, Watanapokasin R (2022) Effects of Artonin E on cell growth inhibition and apoptosis induction in colon cancer LoVo and HCT116 cells. *Molecules* 27:2095.
- Wiley SR, Schooley K, Smolak PJ, Din WS, Huang CP, et al. (1995) Identification and characterization of a new member of the TNF family that induces apoptosis. *Immunity* 3:673-82.
- Pitti RM, Marsters SA, Ruppert S, Donahue CJ, Moore A, et al. (1996) Induction of apoptosis by Apo-2 ligand, a new member of the tumor necrosis factor cytokine family. *J Biol Chem* 271:12687-90.
- Ashkenazi A (2002) Targeting death and decoy receptors of the tumour-necrosis factor superfamily. *Nat Rev Cancer* 2:420-30.
- Siegmund D, Mauri D, Peters N, Juo P, Thome M, et al. (2001) Fas-associated death domain protein (FADD) and caspase-8 mediate up-regulation of c-Fos by Fas ligand and TRAIL via a FLIP-regulated pathway. *J Biol Chem* 276:32585-91.
- Pan G, Ni J, Wei YF, Yu G, Gentz R, et al. (1997) An antagonist decoy receptor and a death domain-containing receptor for TRAIL. *Science* 277:815-8.
- Sheridan JP, Marsters SA, Pitti RM, Gurney A, Skubatch M, et al. (1997) Control of TRAIL-induced apoptosis by a family of signaling and decoy receptors. *Science* 277:818-21.
- Ganten TM, Haas TL, Sykora J, Stahl H, Sprick MR, et al. (2004) Enhanced caspase-8 recruitment to and activation at the DISC is critical for sensitisation of human hepatocellular carcinoma cells to TRAIL-induced apoptosis by chemotherapeutic drugs. *Cell Death Differ* 11:S86-96.
- Li P, Nijhawan D, Budihardjo I, Srinivasula SM, Ahmad M, et al. (1997) Cytochrome c and dATP-dependent formation of Apaf-1/caspase-9 complex initiates an apoptotic protease cascade. *Cell* 91:479-89.
- Wei MC, Lindsten T, Mootha VK, Weiler S, Gross A, et al. (2000) tBID, a membrane-targeted death ligand, oligomerizes BAK to release cytochrome c. *Genes Dev* 14:2060-71.
- Grinberg M, Sarig R, Zaltsman Y, Frumkin D, Grammatikakis N, et al. (2002) tBID homooligomerizes in the mitochondrial membrane to induce apoptosis. *J Biol Chem* 277:12237-45.
- Logue SE, Cleary P, Saveljeva S, Samali A (2013) New directions in ER stress-induced cell death. *Apoptosis* 18:537-46.
- Eskes R, Desagher S, Antonsson B, Martinou JC (2000) Bid induces the oligomerization and insertion of Bax into the outer mitochondrial membrane. *Mol Cell Biol* 20:929-35.
- Baliga B, Kumar S (2003) Apaf-1/cytochrome c apoptosome: an essential initiator of caspase activation or just a sideshow? *Cell Death Differ* 10(1):16-8.
- Bonavida B, Ng CP, Jazirehi A, Schiller G, Mizutani Y (1999) Selectivity of TRAIL-mediated apoptosis of cancer cells and synergy with drugs: the TRAIL to non-toxic cancer therapeutics. *Int J Oncol* 15(4):793-802.
- Oh Y, Swierczewska M, Kim TH, et al. (2015) Delivery of tumor-homing TRAIL sensitizer with long-acting TRAIL as a therapy for TRAIL-resistant tumors. *J Control Release* 220:671-81.
- Yagolovich AV, Gasparian ME, Dolgikh DA (2023) Recent advances in the development of nanodelivery systems targeting the TRAIL death receptor pathway. *Pharmaceutics* 15:515.
- Kelley SK, Harris LA, Xie D, et al. (2001) Preclinical studies to predict the disposition of Apo2L/TRAIL in humans: characterization of in vivo efficacy, pharmacokinetics, and safety. *J Pharmacol Exp Ther* 299:31-8.
- Dimberg LY, Anderson CK, Camidge R, Behbakht K, Thorburn A, et al. (2013) On the TRAIL to successful cancer therapy? Predicting and counteracting resistance against TRAIL-based therapeutics. *Oncogene* 32:1341-50.
- Thorburn A, Behbakht K, Ford H (2008) TRAIL receptor-targeted therapeutics: resistance mechanisms and strategies to avoid them. *Drug Resist Updat* 11:17-24.
- Zhang L, Fang B (2005) Mechanisms of resistance to TRAIL-induced apoptosis in cancer. *Cancer Gene Ther* 12:228-37.
- Wang H, Davis JS, Wu X (2014) Immunoglobulin Fc domain fusion to TRAIL significantly prolongs its plasma half-life and enhances its antitumor activity. *Mol Cancer Ther* 13:643-50.
- Hutt M, Fellermeier-Kopf S, Seifert O, Schmitt LC, Pfizenmaier K, et al. (2018) Targeting scFv-Fc-scTRAIL fusion proteins to tumor cells. *Oncotarget* 9:11322-35.
- Hutt M, Marquardt L, Seifert O, et al. (2017) Superior properties of Fc-comprising scTRAIL fusion proteins. *Mol Cancer Ther* 16:2792-802.

27. Kontermann RE (2011) Strategies for extended serum half-life of protein therapeutics. *Curr Opin Biotechnol* 22:868-76.
28. Roopenian DC, Akilesh S (2007) FcRn: the neonatal Fc receptor comes of age. *Nat Rev Immunol* 7:715-28.
29. Thanaketpaisarn O, Waiwut P, Sakurai H, Saiki I (2011) Artesunate enhances TRAIL-induced apoptosis in human cervical carcinoma cells through inhibition of the NF- $\kappa$ B and PI3K/Akt signaling pathways. *Int J Oncol* 39:279-85.
30. Haynes RK (2001) Artemisinin and derivatives: the future for malaria treatment? *Curr Opin Infect Dis* 14:719-26.
31. Niederreiter M, Klein J, Arndt K, Werner J, Mayer B (2023) Anti-cancer effects of artesunate in human 3D tumor models of different complexity. *Int J Mol Sci* 24:7844.
32. Efferth T (2017) From ancient herb to modern drug: Artemisia annua and artemisinin for cancer therapy. *Semin Cancer Biol* 46:65-83.
33. Abbasi-Malati Z, Khanicheragh P, Narmi MT, et al. (2024) Tumoroids, a valid preclinical screening platform for monitoring cancer angiogenesis. *Stem Cell Res Ther* 15:267.
34. Abbas ZN, Al-Saffar AZ, Jasim SM, Sulaiman GM (2023) Comparative analysis between 2D and 3D colorectal cancer culture models for insights into cellular morphological and transcriptomic variations. *Sci Rep* 13:18380.
35. Chen L, Wei X, Gu D, Xu Y, Zhou H (2023) Human liver cancer organoids: biological applications, current challenges, and prospects in hepatoma therapy. *Cancer Lett* 555:216048.
36. Xue Y, Zhao Y, Yan S, et al. (2025) IL-1 $\beta$  induced intestinal inflammation pathogenesis in East Friesian sheep: insights from organoid modeling. *Animals* 15:1097.
37. Hong SH, Lee DH, Lee YS, et al. (2018) Correction: Molecular crosstalk between ferroptosis and apoptosis: emerging role of ER stress-induced p53-independent PUMA expression. *Oncotarget* 9:24869.
38. Kalimuthu K, Kim JH, Park YS, et al. (2021) Glucose deprivation-induced endoplasmic reticulum stress response plays a pivotal role in enhancement of TRAIL cytotoxicity. *J Cell Physiol* 236:6666-77.
39. Kim JH, Najy AJ, Li J, Chen J, Choudry MHA, et al. (2022) Involvement of Bid in the crosstalk between ferroptotic agent-induced ER stress and TRAIL-induced apoptosis. *J Cell Physiol* 237:4180-96.
40. Song JJ, An AJ, Kwon YT, Lee YJ (2007) Evidence for two modes of development of acquired TRAIL resistance: involvement of Bcl-xL. *J Biol Chem* 282:319-28.
41. Gleeson EM, Feldman R, Mapow BL, et al. (2018) Appendix-derived pseudomyxoma peritonei: molecular profiling toward treatment of a rare malignancy. *Am J Clin Oncol* 41:777-83.
42. Weeber F, Ooft SN, Dijkstra KK, Voest EE (2017) Tumor organoids as a pre-clinical cancer model for drug discovery. *Cell Chem Biol* 24:1092-100.
43. Edmondson R, Broglie JJ, Adcock AF, Yang L (2014) Three-dimensional cell culture systems and their applications in drug discovery and cell-based biosensors. *Assay Drug Dev Technol* 12:207-18.
44. Efferth T, Sauerbrey A, Olbrich A, et al. (2003) Molecular modes of action of artesunate in tumor cell lines. *Mol Pharmacol* 64:382-94.
45. Wang S, El-Deiry WS (2003) TRAIL and apoptosis induction by TNF-family death receptors. *Oncogene* 22:8628-35.
46. Huang QF, Li YH, Huang ZJ, et al. (2023) Artesunate carriers induced ferroptosis to overcome biological barriers for anti-cancer. *Eur J Pharm Sci* 190:284-93.